Journal of Molecular Graphics and Modelling 28 (2009) 305–312

Contents lists available at ScienceDirect

Journal of Molecular Graphics and Modelling

journal homepage: www.elsevier.com/locate/JMGM

Structural features and dynamics properties of human apolipoprotein A-I in a model of synthetic HDL

Alessandro Guerini Rocco [a], Elisabetta Gianazza [a], Laura Calabresi [b], Cristina Sensi [a], Guido Franceschini [b], Cesare R. Sirtori [a,b], Ivano Eberini [a,b,*]

[a] Gruppo di Studio per la Proteomica e la Struttura delle Proteine, Dipartimento di Scienze Farmacologiche, Università degli Studi di Milano, via Giuseppe Balzaretti 9, 20133 Milano, Italy
[b] Centro E. Grossi Paoletti, Dipartimento di Scienze Farmacologiche, Università degli Studi di Milano, via Giuseppe Balzaretti 9, 20133 Milano, Italy

ARTICLE INFO

Article history:
Received 18 May 2009
Received in revised form 14 August 2009
Accepted 18 August 2009
Available online 27 August 2009

Keywords:
Lipoprotein
Molecular dynamics
Molecular docking
Essential dynamics
Molecular modeling

ABSTRACT

High-density lipoproteins (HDL) play a major role in the reverse transport of cholesterol and have antiatherogenic activities. Their major protein component is apolipoprotein (apo) A-I. While apoA-I amphipathic α-helix based secondary structure has been extensively investigated, for its lipid-bound tertiary structure only theoretical models have been proposed. In the past years, experimental approaches aimed at a direct visualization of HDL structure have been exploited, but data obtained through different microscopy techniques are conflicting and do not settle the issue. Here we present a 50 ns molecular dynamics simulation of a synthetic HDL containing two molecules of apoA-I and 101 of L-α-palmitoyl-oleoyl-phosphatidylcholine.

Essential dynamics and structural property investigations suggest that the stabilization of the system is obtained through specific motions, whose driving forces are protein–phospholipid interactions. The most important are: the relative sliding of the two apoA-I molecules along their major axes, the relative rotation of the protein chains, and the out-of-plane deformation around proline hinges. The sliding and the out-of-plane deformation allow apoA-I to optimize its interactions with phospholipids, while the rotation is useful to maximize protein–protein salt bridges. The correspondence between computed parameters and their experimental counterparts contributes to validate our model and its dynamic behaviors.

Our findings help in defining a molecular model for apoA-I contained in HDL and suggest a possible mechanism through which apoA-I can vary its diameter and accommodate different numbers of phospholipids during the metabolism of HDL.

1. Introduction

High-density lipoproteins (HDL), the smallest and densest lipoproteins, are the vehicle of the reverse transport of cholesterol and exert antiatherogenic activities [1]. Mature HDL are spherical, whereas nascent HDL are discoidal particles. The major protein component of HDL is apolipoprotein (apo) A-I, representing over 70% of their total protein content.

ApoA-I, present in plasma at 1–1.2 g/L, is a single polypeptide chain of 243 amino acids with a molecular weight of 28 kDa [2,3]. Its structure is composed of a globular N-terminal (residues 1–43) and a lipid-binding C-terminal domain (residues 44–243). The latter consists of ten class A amphipatic α-helices, punctuated at regular intervals by proline residues; eight of these helices are 22 residues in length, whereas two are 11 residue long [4,5]. Two crystal structures for lipid-free apoA-I have been proposed in 1997 [6] and in 2006 [7], but it is well known that this amphipatic protein, as well as all other apolipoproteins, is well structured and exerts its activity only in a lipid environment [8]. Up to now no experimental structure at atomic resolution of lipid-bound apoA-I is available. While apoA-I amphipathic α-helix based secondary structure has been extensively investigated, for its lipid-bound tertiary structure only theoretical models have been proposed. In the picket-fence model [9] the helices run antiparallel to one another (intramolecular protein–protein interactions) and parallel to the lipid acyl chains; in the belt (or rail-fence) model [2], the helices run perpendicular to phospholipids (intermolecular protein–protein interactions). In the hairpin folding [10,11] most helices are perpendicular to the phospholipid acyl chains and with a random head-to-tail and head-to-head arrangement of the two

* Corresponding author at: Dipartimento di Scienze Farmacologiche, Via Giuseppe Balzaretti, 9, 20133 Milano, Italia. Tel.: +39 02 50318280; fax: +39 02 50318284.
E-mail address: ivano.eberini@unimi.it (I. Eberini).

1093-3263/$ – see front matter © 2009 Elsevier Inc. All rights reserved.
doi:10.1016/j.jmgm.2009.08.008

apoA-I molecules. Currently, the most credited model is the belt, but no definitive experimental evidence has been obtained. In the past years, experimental approaches aimed at a direct visualization of HDL structure have been exploited, but data obtained through different microscopy techniques are conflicting and led to alternative models [12,13], so until a HDL would be crystallized the field is open to further model proposals.

For exerting its activity, apoA-I must have a flexible structure, since it is able to accommodate a different number of phospholipids during the changes in HDL size induced by lipoprotein metabolism [13–15]. Synthetic HDL (s-HDL) containing two molecules of apoA-I and a small amount of a homogeneous phospholipid, such as L-α-palmitoyl-oleoyl-phosphatidylcholine (POPC), are widely used as a model of nascent HDL, since they are well characterized and exhibit some of the properties of their physiological counterpart [16].

In the present paper, we focused our attention on structural and dynamics properties of a s-HDL containing two molecules of apoA-I and 101 of POPC as a phospholipid bilayer. To build this model, we applied bioinformatics/computational tools and procedures, starting from one of the already published crystal structures for lipid-free apoA-I [6]. The molecular dynamics (MD) simulation of the resulting macromolecular complex was computed for 50 ns in explicit solvent, gathering data about the behavior of apoA-I in a lipidic environment and sharpening our understanding of its molecular functions in regulating cholesterol homeostasis.

2. Methodology

2.1. Preparation of the apoA-I–apoA-I′ molecule

ApoA-I (PDB ID code: 1AV1, corresponding to amino acids 44–243 of the protein primary structure, solved at 4.0 Å resolution) [6] in two conformations, A and B chains, was docked to another copy of itself by using ZDOCK [17] with default parameters, generating 2000 solutions for each, A–A′, A–B, and B–B′ chain pairs. Chains A and B were selected as inputs because they have a shape dissimilar from one another [6]. The 20 solutions with lowest energy were visually examined. The selection among the solutions of the docking procedure was carried out on the basis of energetic ranking and geometrical considerations (formation of a ring-like structure), as discussed thoroughly in Section 3. The potential energy of the geometrically acceptable structures is reported in Table 1. Only the poses fulfilling the experimental evidence reported in literature for the reciprocal arrangements between protein and lipid components in natural and synthetic HDL were selected and submitted to further computational procedures. Among these requirements we considered essential: an arrangement compatible with a central phospholipid core, the hydrophobic side of apoA-I helices directly in contact with the phospholipid acylic chains, and hydrophilic side of the helices exposed to the solvent. Furthermore several literature data suggest that the apoA-I monomers interact and are stabilized by interchain salt bridge formation: these restraints have been carefully considered both during the visual inspection and during the energy evaluations. On these bases, 5 solutions for the A–A′, 5 for the A–B, and 4 for the B–B′ pairing were selected and subjected to energy minimization (EM) down to a root mean square (RMS) gradient of 0.001 kcal/mol Å with MOE (Chemical Computing Group, Quebec, Canada), using the CHARMM27 force field; a distance-dependent dielectric term was applied. After EM the complexes with the lowest total energy for each of the three chain pairings were selected and submitted to MD simulations of 5 ns each, with implicit solvent. The lengths of the bonds involving the hydrogen atoms were constrained according to the SHAKE algorithm, allowing for an integration time step of 2 fs. The velocities at 300 K were randomly assigned from the Maxwell–Boltzmann distribution. Helical restraints were set as 2.7 Å minimal- and 3.0 Å maximal-allowed distance between the backbone oxygen atom of residue i and the backbone nitrogen atom of residue $i+4$. As reported in literature [18,19], the application of these intra-helical distance restraints is useful for preserving the secondary structure of α-helices by reducing the system degrees of freedom. After removing intra-helical distance restraints, a final EM was performed as described above; the potential energy of the three structures is reported in Table 1. EM and MD were carried out with MOE on a SUN Ultra 40 workstation running CentOS Linux 4.4. Another apoA-I structure (PDB ID code: 2A01) [7] is available since 2006, but because of its four-helix bundle structure it is unsuitable to accommodate lipid molecules. In order to evaluate the possibility for building a s-HDL by using this recent structure, we computed its MD for 6 ns in explicit solvent with the software package GROMACS 3.3.1. Despite this investigatory simulation, the protein did not assume a conformation suitable for accommodating and surrounding the phospholipid core (please, see Section 3).

Table 1
Ranking of the energetically favored structures for apoA-I–apoA-I′ model.

Dimer type	#	Total energy after EM (kJ mol^{-1})	Total energy after MD-EM (kJ mol^{-1})
A–A′	1	−5294.48	
	4	−8149.30	−25404.6
	6	−7055.61	
	17	−3144.93	
	20	−8055.50	
A–B	1	−5711.96	
	3	unstable[a]	
	13	−7987.67	
	14	−9637.47	−26212.1
	17	−2132.21	
B–B′	1	−9587.39	−26624.6
	2	−8643.60	
	5	unstable[a]	
	14	−4672.57	

[a] Total energy after EM > 0.

2.2. Preparation and MD of the s-HDL particle

In order to ensure that the change from an implicit- to an explicit-solvent simulation force field (optimized for lipid properties) did not alter the relative energy ranking of the investigated apoA-I–apoA-I′ model structures computed through the implicit solvent simulations, also the worst energy scoring complex (A–A′ 4) was simulated for 1 ns. During this short MD, the system containing the A–A′ complex always showed a total energy definitely more unfavorable than the system containing the B–B′ complex. Because, according to the energy evaluations carried out through all the selected force fields, the s-HDL containing the B–B′ non-covalent homodimer consistently emerged as the most energetically favored, it was the only assembly considered for the production simulation of the further analyses. The preparation of the s-HDL particle required a large and equilibrated double layer of POPC: a 64 × 64 lipid molecules equilibrated bilayer was obtained from the database of bilayer structures of Peter Tieleman (http://moose.bio.ucalgary.ca), and used to create a larger bilayer of 1008 × 1008 POPC molecules. This novel membrane structure was solvated with water in a 25 nm × 25 nm × 25 nm box and energy-minimized, then its dynamics was simulated for 2 ns in order to get an equilibrated structure and to avoid any boundary artifact. The apoA-I–apoA-I′ docked assembly was placed into the double layer while getting as many lipid molecules as possible

trapped into the hole formed by the ring-like structure, in agreement with relevant experimental data about s-HDL composition [20]. The lipid molecules remaining outside the hole were manually removed using MOE, running on a SGI Fuel workstation, with the aid of Stereo Graphics Crystal Eyes stereo view. The resulting s-HDL particle, containing 101 POPC molecules, was inserted in a 15 nm × 15 nm × 15 nm box that was solvated with simple point charge (SPC) water model. The system was neutralized by adding 12 Na^+ ions, minimized and then simulated in two different steps: (a) 1 ns of position-restrained MD with an isotropic force (1000 kJ mol^{-1} nm^{-2}) applied to all protein atoms in order to allow for both water exit from the hydrophobic bilayer core and solvent relaxation; (b) 50 ns of unrestrained MD. Analysis of the trajectory was performed on the unrestrained MD. The software package GROMACS 3.3.1 [21–23] was used, both on local SUN Ultra 40 workstations running CentOS Linux 4.4 for few ns trial runs and on the Golgi Linux supercomputer at CILEA (Consorzio Interuniversitario Lombardo per l'Elaborazione Automatica) for the main simulation. The GROMOS96 force field, modified according to Berger et al. [24] to improve lipid properties, was applied. All the simulations were performed at 300 K and 1 bar with coupling constant of 0.1 ps for temperature and 1.0 ps for pressure, in both cases applying the Berendsen weak coupling algorithms [25]. The time step for integration was set at 0.002 ps. Fast Particle-Mesh Ewald (PME) electrostatics [26,27] was applied with the following parameters: distance for the Lennard–Jones cutoff = 0.9 nm; distance for the Coulomb cutoff = 0.9 nm; maximum spacing for the Fast Fourier Transform (FFT) grid = 0.12 nm and a cubic interpolation order, with neighbor list searching (updated every 10 steps). Essential dynamics analysis was performed using the Dynatraj service [28]. Energy drift was calculated by performing a least squares quadratic fit of the data to a straight line, and total energy drift was obtained multiplying energy drift by total simulation time. From MD data the fraction of exposed aromatic amino acids, f_a, was obtained according to the following equation:

$$f_a ai = \frac{\langle SAS_{MAX} ai(c)\rangle - \langle SASai(c)\rangle}{\langle SAS_{MAX} ai(c)\rangle} \quad (1)$$

in which $SAS_{MAX}ai(c)$ is the maximum solvent accessible area (*SAS*) value for the side chain of the amino acid *ai*, obtained not taking into account its interactions with other atoms of the simulated system, if the protein were fixed in the conformation *c*; $SASai(c)$ is the real *SAS* value for the side chain of the amino acid *ai* if the protein were fixed in the conformation *c*. The f_a term computed for tryptophan residues can be directly compared with values from tryptophan fluorescence. In the experiments the analysis of quenching data is usually performed according to the Stern–Volmer equation as modified by Lehrer [29]:

$$\frac{F_0}{\Delta F} = \frac{1}{f_a} + \frac{1}{f_a K_s [KI]} \quad (2)$$

3. Results and discussion

Before starting with presentation of results, it is necessary to outline the peculiarities and the limitations of a s-HDL based on the available structural data. No structures for apoA-I in a phospholipidic environment are available at atomic resolution. Even if a small part of apoA-I in SDS has been already characterized by NMR, no evaluations have been carried out of the whole apoA-I molecule with the same experimental approach. X-ray crystallography was successfully applied to obtain the three-dimensional arrangement of this apolipoprotein with varying resolution. Despite the better resolution and the complete coverage of apoA-I primary structure, the crystal obtained by Ajees et al. [7] resembles a lipid-free conformation, characterized by an aggregated/fibrillar structure and did not assume a suitable conformation for proper interactions with phospholipids even after 6 ns MD (Suppl. Fig. SA1). Data on this crystal structure are useful for proposing "a model for transformation of the lipid-free conformation to the high-density lipoprotein-bound form", but not for building a s-HDL that corresponds to the experimental evidence for HDL structure. For these reasons we discarded the more recent and resolved (2.4 Å) apoA-I structure and chose the older one even if solved with a low resolution (4.0 Å). Since the discussion about the tertiary structure arrangement of apoA-I in HDL is not closed yet, as we reported in Section 1, we deem that the 4.0 Å resolution structure deposited by Borhani et al. [6] is not a real limitation for its use in this computational work, and that the apoA-I conformation in this crystal is the only suitable for modeling the interactions between apoA-I and phospholipids. Furthermore, because of intrinsic limitations of the current MD simulations, we decided to set-up our system starting from crystallographic experimental data and not from conformations produced by previous computational procedures, avoiding the risk of a starting bias that can seriously affect the results.

Fig. 1 outlines the steps we followed when building *in silico* a model for s-HDL and shows, from left to right, the structure after protein–protein docking (two apoA-I chains from the lipid-free crystal structure), after assembling with an equilibrated POPC bilayer and at the end of 50 ns MD. Considering the evolution with time of the main structural and energetic parameters of the system during MD, all values appear to plateau in the first part of the simulation (for all the considered parameters, within the first 10 ns).

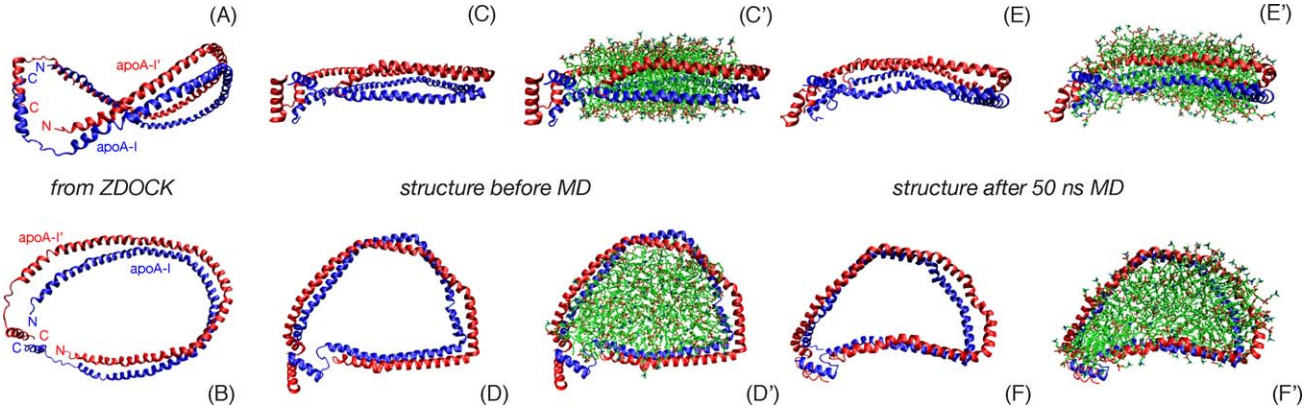

Fig. 1. Steps in model building. (A and B) Structures after the protein–protein docking; (C and C′, D and D′) before MD and (E and E′, F and F′) after 50 ns of MD (color code: blue for apoA-I, red for apoA-I′). Protein structures are rendered as α-carbon ribbon, POPC in CPK colors.

As measured by α-carbon RMSD, 80% of the backbone net displacement is observed during the first 10 ns of the simulation (Fig. 2 panel A); after this time the relaxation from a solid, lipid-free to a solvated, lipid-bound configuration can be considered almost complete. Radius of gyration decreases down to its minimal stable value of approximately 4.2 nm after 4 ns; this size is fully compatible with the properties of s-HDL containing two apoA-I molecules, as known from literature data [30,31]. Considering the *x*, *y*, *z* components of gyration radius, our s-HDL model shows a major and a minor axis of approximately 8.2 and 7.3 nm (Fig. 2 panel B). During the MD simulation, no POPC molecules move away from the s-HDL. The number of hydrogen bonds between the protein chains sharply decreases from the starting value of 480 during the first 200 ps of simulation, and then fluctuates around a value of 362 (Fig. 2 panel C). This behavior is possibly due to the procedure we used to build the s-HDL: in the MD carried out with helical restraints we observe the formation of all the hydrogen bonds theoretically predicted and allowed for apoA-I. Some of these bonds are rapidly lost in the early phase of the main simulation of the s-HDL particle in explicit water. Fig. 2 panel D shows the number of hydrogen bonds between protein and lipids, which keeps growing till approximately 10 ns, to reach at 50 ns a value of 103. Both the protein–protein Coulomb and Lennard–Jones short-range energies change by less than 2% with respect to their starting values during the simulation time, with total drifts of, respectively, 370.4 kJ mol^{-1} and 274.2 kJ mol^{-1}. The reported energy variations are observed mainly during the first part (5 ns) of the trajectory, and this is likely due to the loss of some hydrogen bonds formed during the set-up MD simulation (please, see above). The lipid–lipid Coulomb and Lennard–Jones short-range energies increase, respectively, by <7% and <3% with respect to their values at the start of the MD, with total drifts of 404.6 kJ mol^{-1} and 427.1 kJ mol^{-1}. Conversely, as reported in Fig. 2 panel E, the protein–lipid interaction energies decrease with respect to their starting values by 214% for short-range Coulomb and by 42% for short-range Lennard–Jones energies (total drifts of −2088 kJ mol^{-1} and −2008 kJ mol^{-1}, respectively); a plateau is reached after ca. 9 ns. These energetical evaluations suggest that the increasing number of favorable interactions between proteins and POPC acts as a relevant driving force for the structural reorganization and stabilization of the s-HDL during the simulated time. The number of amino acids in secondary structure (α-helix) slightly changes during the MD (Fig. 2 panel F), and it is close to the value computed for the starting crystal structure. A DSSP run [32] on the minimized last time frame detects in our model 345 amino acids in α-helix, corresponding to 75% over a total of 486 amino acids. This value is in agreement with the one obtained by far-ultraviolet circular dichroism spectra carried out on s-HDL containing apoA-I [33]. The PDB structure we used in this study is a Δ43 apoA-I, so for the first 43 amino acids we assumed that 10 are in α-helix according to the UniProt Knowledgebase (please, look at UniProtKB/Swiss-Prot P02647). The use of this truncated form of apoA-I is suitable for our modeling procedure, since it has been demonstrated that, in HDL with a Stokes diameter below 11 nm, the first 43 amino acids have no interaction with the lipids and are unessential for lipoprotein formation [34]. In Fig. 2 panel G the plot of RMSF, calculated only on the part of MD in which the relaxation from lipid-free crystal to lipid-bound conformation was finished (from 12 to 50 ns), shows peaks of fluctuation corresponding to N- and C-termini of both apoA-I chains whereas the other parts of apoA-I are only slightly flexible. Tryptophan fluorescence polarization at 280 nm depends on the mobility of the side chains, whereas the quenching of intrinsic fluorescence by KI is related to the average environment of the tryptophan residues. As detailed under Section 2, the analysis of quenching data is usually performed according to the Stern–Volmer equation; a f_a term is calculated corresponding to the fraction of exposed tryptophan residues. Table 2 lists the average f_a values for each aromatic amino acid in apoA-I, computed only from 12 to 50 ns. The f_a value we obtained from our simulation for tryptophan (0.60) is consistent with f_a value experimentally measured by Jonas *et al.* for s-HDL with size and composition

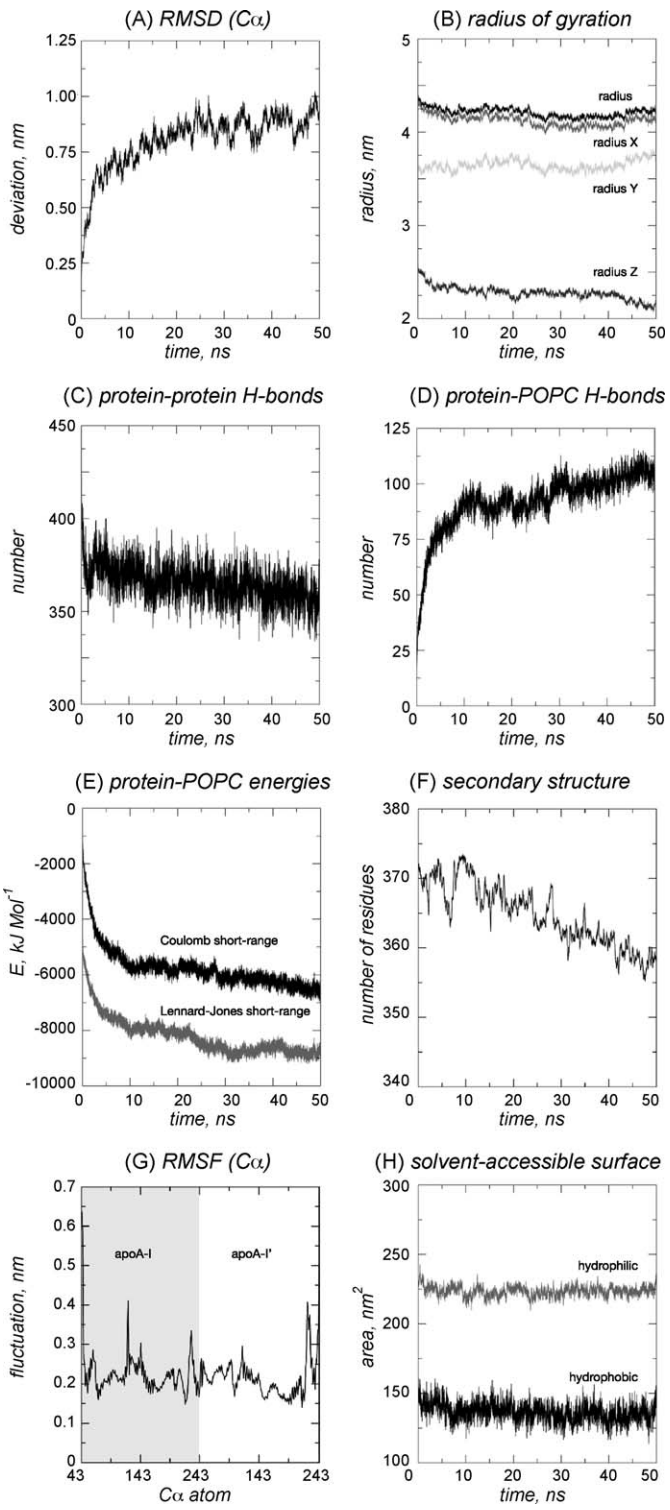

Fig. 2. Structural and energetical parameters. (A) RMSD computed on α-carbons; (B) radius of gyration and its decomposition along cartesian axes; (C) number of protein–protein hydrogen bonds; (D) number of protein–lipid hydrogen bonds; (E) Coulomb short-range and Lennard–Jones short-range protein–lipid interaction energies; (F) total number of structured residues; (G) RMSF calculated from 12 to 50 ns: amino acid numbering is according to the primary structure of apoA-I (grey background) and apoA-I′ (white background); (H) hydrophobic and hydrophilic lipid SAS.

Table 2
Average SAS_{MAX}, SAS, and f_a values ± S.D. for each aromatic amino acid calculated from 12 to 50 ns.

Chain	Amino acid	$\langle SAS_{MAX}(c)\rangle$ (nm^2)	$\langle SAS(c)\rangle$ (nm^2)	f_a
apoA-I	W^{50}	2.55 ± 0.11	1.50 ± 0.86	0.41 ± 0.34
	W^{72}	2.54 ± 0.11	1.09 ± 0.91	0.57 ± 0.36
	W^{108}	2.54 ± 0.11	0.90 ± 0.73	0.65 ± 0.29
apoA-I′	W^{50}	2.54 ± 0.11	0.90 ± 0.72	0.65 ± 0.28
	W^{72}	2.55 ± 0.11	0.90 ± 0.70	0.65 ± 0.27
	W^{108}	2.53 ± 0.11	0.87 ± 0.68	0.66 ± 0.27
apoA-I	F^{57}	2.17 ± 0.11	0.92 ± 0.73	0.58 ± 0.34
	F^{71}	2.17 ± 0.11	0.82 ± 0.72	0.62 ± 0.33
	F^{104}	2.16 ± 0.10	0.58 ± 0.53	0.73 ± 0.25
	F^{225}	2.17 ± 0.10	0.63 ± 0.59	0.71 ± 0.27
	F^{229}	2.17 ± 0.10	0.65 ± 0.59	0.70 ± 0.27
apoA-I′	F^{57}	2.16 ± 0.10	0.65 ± 0.56	0.70 ± 0.26
	F^{71}	2.16 ± 0.11	0.67 ± 0.57	0.69 ± 0.26
	F^{104}	2.16 ± 0.10	0.66 ± 0.56	0.69 ± 0.26
	F^{225}	2.16 ± 0.11	0.67 ± 0.54	0.69 ± 0.25
	F^{229}	2.16 ± 0.10	0.67 ± 0.56	0.69 ± 0.26
apoA-I	Y^{100}	2.26 ± 0.11	0.63 ± 0.56	0.72 ± 0.25
	Y^{115}	2.26 ± 0.10	0.73 ± 0.62	0.68 ± 0.27
	Y^{166}	2.27 ± 0.10	0.65 ± 0.60	0.71 ± 0.26
	Y^{192}	2.28 ± 0.10	0.72 ± 0.63	0.68 ± 0.28
	Y^{236}	2.27 ± 0.11	0.73 ± 0.62	0.68 ± 0.27
apoA-I′	Y^{100}	2.27 ± 0.11	0.72 ± 0.61	0.68 ± 0.27
	Y^{115}	2.27 ± 0.10	0.70 ± 0.58	0.69 ± 0.26
	Y^{166}	2.26 ± 0.11	0.71 ± 0.58	0.69 ± 0.26
	Y^{192}	2.27 ± 0.10	0.75 ± 0.61	0.67 ± 0.27
	Y^{236}	2.26 ± 0.11	0.72 ± 0.59	0.68 ± 0.26

similar to our model (please, see "degree of Trp accessibility" raw for r-HDL-2 + 3 in Table 2 [30]; f_a column for r-HDL-97 in Table 2 [35]; and f_a column for 78-Å r-HDL and 93-Å r-HDL in Table 2 [36]). While the spectroscopic methods only provide average estimates for the measured parameter, the molecular modeling approach allows singling out individual contributions. According to our simulation, computed f_a values for individual tryptophan residues span from a minimum of 0.41 to a maximum of 0.66, suggesting a different involvement of their side chains in the interaction with POPC and protein chains. The average f_a for phenylalanine and tyrosine are, respectively, 0.68 and 0.69; since these amino acids are not amenable to fluorescence analysis, such result cannot have an experimental counterpart.

The most credited model for apoA-I bound to lipids, the double belt, is supported by the role of salt bridges and the stacking of proline residues [2,37,38]. Even if obtained through a totally different procedure, our model shares several structural properties with the model of Segrest et al. [2,38]. Table 3 lists the salt bridges between the two apolipoprotein chains, computed from 12 to 50 ns. Among 10 salt bridges identified, 8 involve the same partners as in Segrest's model, as reported in Table 3. At the beginning of our simulation the two apolipoprotein molecules, apoA-I and apoA-I′, run antiparallel, with helix 4 of apoA-I associated to helix 6 of apoA-I′, helix 6 of apoA-I to helix 4 of apoA-I′, and the two helices 5 close together, and four prolines are juxtaposed (apoA-I P^{99}–apoA-I′ P^{165}, apoA-I P^{121}–apoA-I′ P^{143}, apoA-I P^{143}–apoA-I′ P^{121} and apoA-I P^{165}–apoA-I′ P^{99}) (see Fig. 3 panel A). The arrangement of the two apoA-I is thus very similar to the K^{133}/K^{133} rotamer proposed by Klon et al. [38], with the K^{133} of the two apoA-I chains aligned, and with an LL5/5 spatial

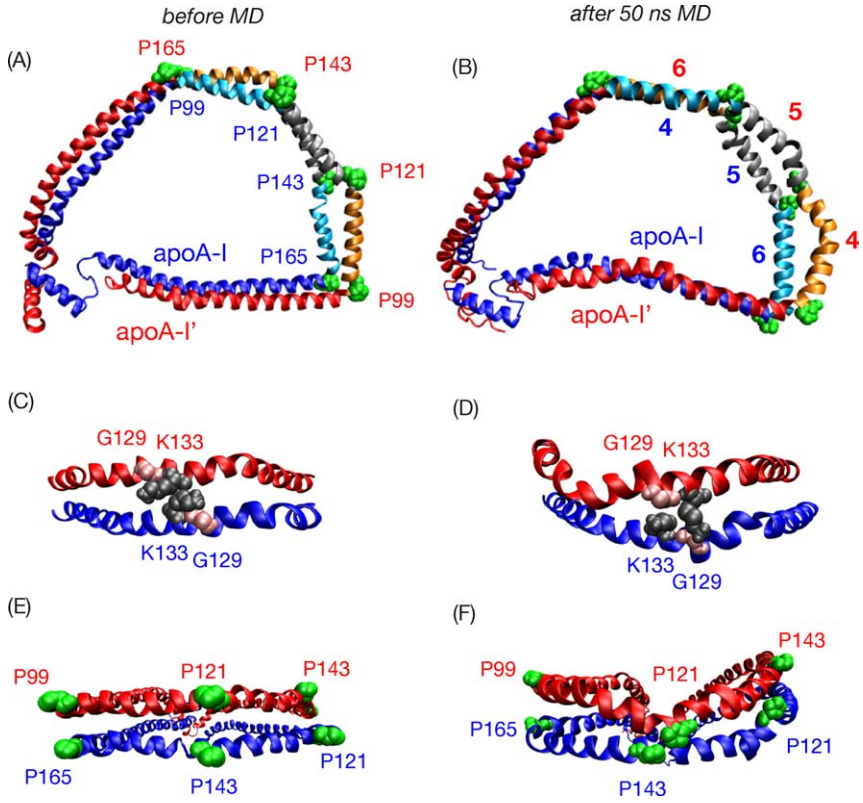

Fig. 3. Structural properties of the s-HDL. Structural properties for apoA-I–apoA-I′ in s-HDL. (A, C, E) before MD; (B, D, F) after 50 ns of MD (color code: blue for apoA-I, red for apoA-I′). Protein structure is rendered as α-carbon ribbon, selected amino acids in VDW. Panels A, B show the relative alignment of the two apolipoproteins, with helical repeats 4, 5 and 6 rendered in different colors. The four stacked proline pairs are colored in green. Panels C, D represent the position of G^{129} and K^{133}. Panels E, F show the out-of-plane deformation around the proline pair apoA-I P^{143} and apoA-I′ P^{121}.

Table 3
Intermolecular salt bridges that remain at a distance ≤0.3 nm from 12 to 50 ns.

apoA-I	apoA-I′
D^{89}	R^{177}
E^{78}	R^{188}
$\underline{D^{89}}$	$\underline{R^{173}}$
$\underline{K^{133}}$	$\underline{E^{125}}$
$\underline{R^{173}}$	$\underline{D^{89}}$
$\underline{E^{111}}$	$\underline{R^{151}}$
R^{151}	E^{111}
R^{177}	D^{89}
R^{177}	E^{85}
E^{92}	R^{173}

The salt bridges not identified in [38] are underlined.

organization [2,38] (Fig. 3 panel C). Comparing s-HDL structure before MD with the one at the end of the simulation, it is clear that the two apoA-I molecules rotate relatively to one another: the C-terminal domain of apoA-I turns towards the N-terminus of apoA-I′. This direction of rotation is the most favorable according to Klon et al. [38] as maximizing protein–protein ionic interactions (salt bridges). According to Klon et al. terminology [38], at the end of our MD simulation, the rotamer conformation can be described as K^{133}/G^{129} (see Fig. 3 panels C and D). G^{129} and K^{133} were chosen just to univocally identify the different apoA-I–apoA-I′ rotamers, and to easily compare Klon's results with ours, not to highlight any of their biological and/or physicochemical functions.

From essential dynamics (ED) analysis (Fig. 4), performed on the part of MD trajectory in which apoA-I changes its conformation from solid lipid-free to solvated lipid-bound (first 5 ns), we obtain 1200 eigenvalues. The first eigenvector (Fig. 4 panel A) accounts for 90% of the total amount of the motions (247.95 nm^2) and describes the relative sliding of the two apoA-I molecules along their major axes. This coordinated motion is clearly the most relevant mechanism for s-HDL diameter modification, which does not explore any of the already reported out-of-plane deformations. The second eigenvector (Fig. 4 panel B), 5.4% of total motion, is a complex modification of the protein structure, which involves an out-of-plane deformation around all the stacked proline hinges, and a movement of approaching to phospholipids. The third and fourth eigenvectors (Fig. 4 panels C and D), accounting only for 1.3% and 0.8% of the total amount of the motions, are out-of-plane deformations around the four hinges formed by proline pairs. The combination of these essential motions leads protein chains to get closer to the POPC core, thus minimizing the solvent accessible area (SAS) of phospholipids; this effect is more evident on the hydrophobic SAS (Fig. 2 panel H). Panels E and F of Fig. 3 show the out-of-plane deformation occurred around the apoA-I P^{143}–apoA-I' P^{121} hinge. On the contrary during the set-up simulation, carried out with MOE, the proteins decrease their out-of-plane deformation with respect to the starting crystal structure, evolving to a planar belt conformation (Fig. 1 panels A–D). The ED analysis on the last part of MD (from 12 to 50 ns) is associated with a total eigenvalue of only 18.11 nm^2, of which only 55% is associated with the first four eigenvectors. These data suggest that apoA-I dynamics after its relaxation period is complex and composed by different principal motions (not shown).

In the past, a rearrangement mechanism for small HDL (with a diameter lower than 10 nm) had been hypothesized; it was supposed that a helical region of apoA-I could hinge off the lipid core [14,34,39], minimizing the phospholipid area exposed to the solvent. This "hinge domain" has to be a stretch with a lower lipid affinity, and some evidence suggests it could correspond to a helical segment localized between helix 4 and 7 [14,31,40,41]. However, the existence of this region is neither definitively

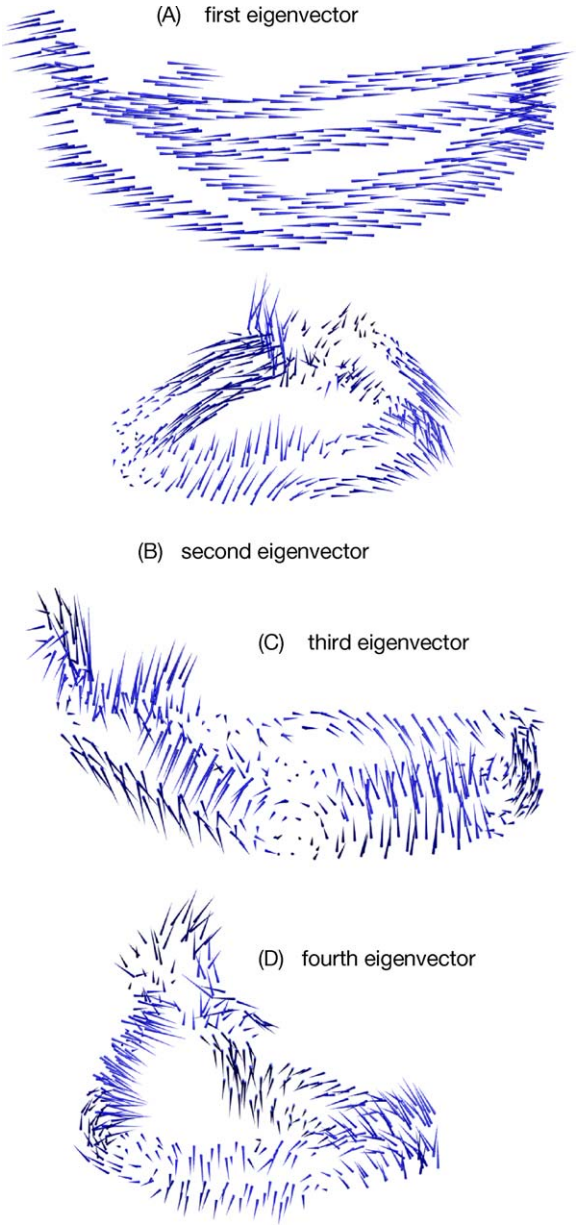

Fig. 4. Essential dynamics performed on the first part of MD (up to 5 ns). (A–D) "Porcupine" plots of the coordinated motions for apoA-I–apoA-I′ in s-HDL. The displacement of α-carbons is projected along the first four eigenvectors. Analysis on the first part of MD (up to 5 ns).

demonstrated nor accurately mapped onto the apoA-I sequence. Furthermore, a recent paper from Catte et al. [13], using both experimental and computational tools, pointed out that the "hinge domain" model is not compatible with very low diameter particles (i.e. around 7.8 nm). The authors studied the modification of apoA-I arrangement during progressive removal of phospholipid molecules: after few nanoseconds of MD, apoA-I remarkably deviated from its original belt conformation to a non-planar, ellipsoidal one, but no "hinge domain" was observed. Our data are consistent with Catte's, but in addition introduce a sliding motion, accounting for as much as 90% of the sum of all eigenvalues. These observations demonstrate that the stabilization of nascent HDL is allowed by the coordinated motions described in Fig. 4, rather than by the presence of a "hinge domain".

In a previous paper from our group [19], we proposed a structure for the heterodimer between apolipoprotein $A\text{-}I_{Milano}$ and apolipoprotein A-II (apoA-I_M–apoA-II) in a s-HDL containing

POPC. We demonstrated that the major susceptibility to proteolysis of the heterodimer compared to the wild type apoA-I is due to different structural and dynamics features. The s-HDL with apoA-I_M–apoA-II has several high RMSF regions, whereas the RMSF plot of the wild type s-HDL shows peaks only at the extremities of the protein chains. We also demonstrated that the high RMSF regions of apoA-I_M–apoA-II correspond to the sites of cleavage by trypsin. Furthermore, apoA-I_M–apoA-II undergoes a decrease in secondary structure during the simulation; on the contrary, no significant changes in secondary structure content are observed in wild type apoA-I. It is well known that a protein with a lower secondary structural content and a higher RMSF becomes more susceptible to proteolysis, as described for delipidated unstructured apoA-I [42].

The correspondence between computed parameters (gyration radius, number of bound phospholipids, total amount of helical structure, f_a values) and their experimental counterparts, retrieved from literature, contributes to validate our model set-up process and the computed dynamic behavior of the studied assembly.

4. Conclusions

From the analysis of the trajectory, we can conclude that the interactions between proteins and POPC are the driving force for the reorganization of the s-HDL. The stabilization of the system is obtained through specific relevant motions: the relative sliding of the two apoA-I molecules along their major axes, the relative rotation of the protein chains and out-of-plane deformations, which lead to a change of the s-HDL size, thus allowing the protein to optimize its interactions with different numbers of phospholipid molecules and maximize the protein–protein ionic interactions. Our findings, together with recent literature data [13,38], suggest a possible mechanism through which apoA-I can rearrange and stabilize its structure, and accommodate a varying number of phospholipids.

Acknowledgements

The authors are grateful to Luca Mollica for fruitful discussions, and to Alessia Caronno for editing the manuscript. The authors wish to thank the CILEA HPC staff for their assistance during calculations on the CILEA cluster.

This investigation was supported in part by a grant from MIUR: FIRB 2003 "Il riconoscimento molecolare nelle interazioni proteina-ligando, proteina-proteina e proteina superficie: sviluppo di approcci sperimentali e computazionali integrati per lo studio di sistemi di interesse farmaceutico".

Appendix A. Supplementary data

Supplementary data associated with this article can be found, in the online version, at doi:10.1016/j.jmgm.2009.08.008.

References

[1] G. Franceschini, P. Maderna, C.R. Sirtori, Reverse cholesterol transport: physiology and pharmacology, Atherosclerosis 88 (1991) 99–107.
[2] J.P. Segrest, M.K. Jones, A.E. Klon, C.J. Sheldahl, M. Hellinger, H. De Loof, S.C. Harvey, A detailed molecular belt model for apolipoprotein A-I in discoidal high density lipoprotein, J. Biol. Chem. 274 (1999) 31755–31758.
[3] R.J. Cushley, M. Okon, NMR studies of lipoprotein structure, Ann. Rev. Biophys. Biomol. Struct. 31 (2002) 177–206.
[4] M.S. Boguski, M. Freeman, N.A. Elshourbagy, J.M. Taylor, J.I. Gordon, On computer-assisted analysis of biological sequences: proline punctuation, consensus sequences, and apolipoprotein repeats, J. Lipid Res. 27 (1986) 1011–1034.
[5] R.T. Nolte, D. Atkinson, Conformational analysis of apolipoprotein A-I and E-3 based on primary sequence and circular dichroism, Biophys. J. 63 (1992) 1221–1239.
[6] D.W. Borhani, D.P. Rogers, J.A. Engler, C.G. Brouillette, Crystal structure of truncated human apolipoprotein A-I suggests a lipid-bound conformation, Proc. Natl. Acad. Sci. U.S.A. 94 (1997) 12291–12296.
[7] A.A. Ajees, G.M. Anantharamaiah, V.K. Mishra, M.M. Hussain, H.M. Murthy, Crystal structure of human apolipoprotein A-I: insights into its protective effect against cardiovascular diseases, Proc. Natl. Acad. Sci. U.S.A. 103 (2006) 2126–2131.
[8] J.P. Segrest, R.L. Jackson, J.D. Morrisett, A.M.J. Gotto, A molecular theory of lipid–protein interactions in the plasma lipoproteins, FEBS Lett. 38 (1974) 247–258.
[9] J.C. Phillips, W. Wriggers, Z. Li, A. Jonas, K. Schulten, Predicting the structure of apolipoprotein A-I in reconstituted high-density lipoprotein disks, Biophys. J. 73 (1997) 2337–2346.
[10] D.P. Rogers, L.M. Roberts, J. Lebowitz, G. Datta, G.M. Anantharamaiah, J.A. Engler, C.G. Brouillette, The lipid-free structure of apolipoprotein A-I: effects of amino-terminal deletions, Biochemistry 37 (1998) 11714–11725.
[11] D.P. Rogers, L.M. Roberts, J. Lebowitz, J.A. Engler, C.G. Brouillette, Structural analysis of apolipoprotein A-I: effects of amino- and carboxy-terminal deletions on the lipid-free structure, Biochemistry 37 (1998) 945–955.
[12] C. Culot, F. Durant, S. Lazarescu, P.A. Thiry, B. Vanloo, M.Y. Rosseneu, L. Lins, R. Brasseur, Structural investigation of reconstituted high density lipoproteins by scanning tunnelling microscopy, Appl. Surf. Sci. 230 (2004) 151–157.
[13] A. Catte, J.C. Patterson, M.K. Jones, W.G. Jerome, D. Bashtovyy, Z. Su, F. Gu, J. Chen, M.P. Aliste, S.C. Harvey, L. Li, G. Weinstein, J.P. Segrest, Novel changes in discoidal high density lipoprotein morphology: a molecular dynamics study, Biophys. J. 90 (2006) 4345–4360.
[14] J.N. Maiorano, R.J. Jandacek, E.M. Horace, W.S. Davidson, Identification and structural ramifications of a hinge domain in apolipoprotein A-I discoidal high-density lipoproteins of different size, Biochemistry 43 (2004) 11717–11726.
[15] C.G. Brouillette, W.J. Dong, Z.W. Yang, M.J. Ray, I.I. Protasevich, H.C. Cheung, J.A. Engler, Forster resonance energy transfer measurements are consistent with a helical bundle model for lipid-free apolipoprotein A-I, Biochemistry 44 (2005) 16413–16425.
[16] G. Rossoni, M. Gomaraschi, F. Berti, C.R. Sirtori, G. Franceschini, L. Calabresi, Synthetic high-density lipoproteins exert cardioprotective effects in myocardial ischemia/reperfusion injury, J. Pharmacol. Exp. Therap. 308 (2004) 79–84.
[17] R. Chen, L. Li, Z. Weng, ZDOCK: an initial-stage protein-docking algorithm, Proteins 52 (2003) 80–87.
[18] R.M. Vitale, C. Pedone, P.G. De Benedetti, F. Fanelli, Structural features of the inactive and active states of the melanin-concentrating hormone receptors: insights from molecular simulations, Proteins 56 (2004) 430–448.
[19] A. Guerini Rocco, L. Mollica, E. Gianazza, L. Calabresi, G. Franceschini, C.R. Sirtori, I. Eberini, A model structure for the heterodimer apoA-IMilano–apoA-II supports its peculiar susceptibility to proteolysis, Biophys. J. 91 (2006) 3043–3049.
[20] L. Calabresi, G. Vecchio, F. Frigerio, L. Vavassori, C.R. Sirtori, G. Franceschini, Reconstituted high-density lipoproteins with a disulfide-linked apolipoprotein A-I dimer: evidence for restricted particle size heterogeneity, Biochemistry 36 (1997) 12428–12433.
[21] H.J.C. Berendsen, D. van der Spoel, R. van Drunen, GROMACS: a message-passing parallel molecular dynamics implementation, Comp. Phys. Commun. 91 (1995) 43–56.
[22] E. Lindahl, B. Hess, D. van der Spoel, GROMACS 3.0: a package for molecular simulation and trajectory analysis, J. Mol. Model. 7 (2001) 306–317.
[23] D. van der Spoel, A.R. van Buuren, E. Apol, P.J. Meulenhoff, D.P. Tieleman, A.L.T.M. Sijbers, K.A. Feenstra, E. Lindhal, R. van Drunen, H.J.C. Berendsen, Gromacs User Manual version 3.0, Nijenborgh 4, 9747 AG Groningen, 2001.
[24] O. Berger, O. Edholm, F. Jahnig, Molecular dynamics simulations of a fluid bilayer of dipalmitoylphosphatidylcholine at full hydration, constant pressure, and constant temperature, Biophys. J. 72 (1997) 2002–2013.
[25] H.J.C. Berendsen, J.P.M. Postma, A. DiNola, J.R. Haak, Molecular dynamics with coupling to an external bath, J. Chem. Phys. 81 (1984) 3684–3690.
[26] T. Darden, D. York, L. Pedersen, Particle mesh Ewald: an N-log(N) method for Ewald sums in large systems, J. Chem. Phys. 98 (1993) 10089–10092.
[27] U. Essmann, L. Perera, M.L. Berkowitz, T. Darden, H. Lee, L.G. Pedersen, A smooth particle mesh Ewald potential, J. Chem. Phys. 103 (1995) 8577–8592.
[28] C.P. Barrett, B.A. Hall, M.E. Noble, Dynamite: a simple way to gain insight into protein motions, Acta Crystallogr. D: Biol. Crystallogr. 60 (2004) 2280–2287.
[29] S.S. Lehrer, Solute perturbation of protein fluorescence. The quenching of the tryptophyl fluorescence of model compounds and of lysozyme by iodide ion, Biochemistry 10 (1971) 3254–3263.
[30] A. Jonas, K.E. Kezdy, H.J. Wald, Defined apolipoprotein A-I conformations in reconstituted high density lipoprotein discs, J. Biol. Chem. 264 (1989) 4818–4824.
[31] L. Calabresi, Q.H. Meng, G.R. Castro, Y.L. Marcel, Apolipoprotein A-I conformation in discoidal particles: evidence for alternate structures, Biochemistry 32 (1993) 6477–6484.
[32] W. Kabsch, C. Sander, Dictionary of protein secondary structure: pattern recognition of hydrogen-bonded and geometrical features, Biopolymers 22 (1983) 2577–2637.
[33] L. Calabresi, G. Vecchio, R. Longhi, E. Gianazza, G. Palm, H. Wadensten, A. Hammarström, A. Olsson, A. Karlström, T. Sejlitz, H. Ageland, C.R. Sirtori, G. Franceschini, Molecular characterization of native and recombinant apolipoprotein A-I_{Milano} dimer: the introduction of an interchain disulfide bridge remarkably alters the physicochemical properties of apolipoprotein A-I, J. Biol. Chem. 269 (1994) 32168–32174.
[34] L. Li, J. Chen, V.K. Mishra, J.A. Kurtz, D. Cao, A.E. Klon, S.C. Harvey, G.M. Anantharamaiah, J.P. Segrest, Double belt structure of discoidal high density lipoproteins: molecular basis for size heterogeneity, J. Mol. Biol. 343 (2004) 1293–1311.
[35] J.H. Wald, E.S. Krul, A. Jonas, Structure of apolipoprotein A-I in three homogeneous, reconstituted high density lipoprotein particles, J. Biol. Chem. 265 (1990) 20037–20043.

[36] A. Jonas, J.H. Wald, K.L.H. Toohill, E.S. Krul, K.E. Kézdy, Apolipoprotein A-I structure and lipid properties in homogeneous, reconstituted spherical and discoidal high density lipoproteins, J. Biol. Chem. 265 (1990) 22123–22129.
[37] C. Sheldahl, S.C. Harvey, Molecular dynamics on a model for nascent high-density lipoprotein: role of salt bridges, Biophys. J. 76 (1999) 1190–1198.
[38] A.E. Klon, J.P. Segrest, S.C. Harvey, Molecular dynamics simulations on discoidal HDL particles suggest a mechanism for rotation in the apo A-I belt model, J. Mol. Biol. 324 (2002) 703–721.
[39] C.G. Brouillette, J.L. Jones, T.C. Ng, H. Kercret, B.H. Chung, J.P. Segrest, Structural studies of apolipoprotein A-I/phosphatidylcholine recombinants by high-field proton NMR, nondenaturing gradient gel electrophoresis, and electron microscopy, Biochemistry 23 (1984) 359–367.
[40] Y.L. Marcel, P.R. Provost, H. Koa, E. Raffai, N.V. Dac, J.C. Fruchart, E. Rassart, The epitopes of apolipoprotein A-I define distinct structural domains including a mobile middle region, J. Biol. Chem. 266 (1991) 3644–3653.
[41] L. Calabresi, G. Tedeschi, C. Treu, S. Ronchi, D. Galbiati, S. Airoldi, C.R. Sirtori, Y. Marcel, G. Franceschini, Limited proteolysis of a disulfide-linked apoA-I dimer in reconstituted HDL, J. Lipid Res. 42 (2001) 935–942.
[42] Y. Ji, A. Jonas, Properties of an N-terminal proteolytic fragment of apolipoprotein A-I in solution and in reconstituted high density lipoproteins, J. Biol. Chem. 270 (1995) 11290–11297.